



Identification and Mitigation of Smoke-Ring Effects in Scintillator-based Electron Beam Images at the European XFEL

G. Kube, A. Novokshonov, S. Liu, M. Scholz
DESY (Hamburg)

- Introduction
- Scintillator Experience from HEP
- Quenching Model for XFEL Measurements
- Conclusion and Outlook

OTR Transverse Beam Profiling

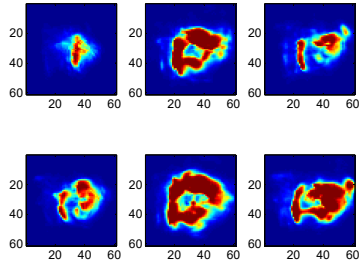
- Optical Transition Radiation (OTR) for beam diagnostics

- backward OTR: reflection of virtual photons
→ instantaneous process
- single shot measurement
- full transverse (2D) profile information

- Coherent OTR observation at LCLS (SLAC)

R. Akre et al., Phys. Rev. ST Accel. Beams **11** (2008) 030703, H. Loos et al., Proc. FEL 2008, Gyeongju, Korea, p.485.

- OTR 12



- OTR 22



measured spot is no beam image!

- strong shot-to-shot fluctuations
- doughnut structure
- change of spectral contents

- interpretation of coherent formation in terms of “Microbunching Instability”

E.L. Saldin et al., NIM **A483** (2002) 516

Z. Huang and K. Kim, Phys. Rev. ST Accel. Beams **5** (2002) 074401

- alternative schemes for beam profile diagnostics

- stochastic radiation emission (destruction of coherence)

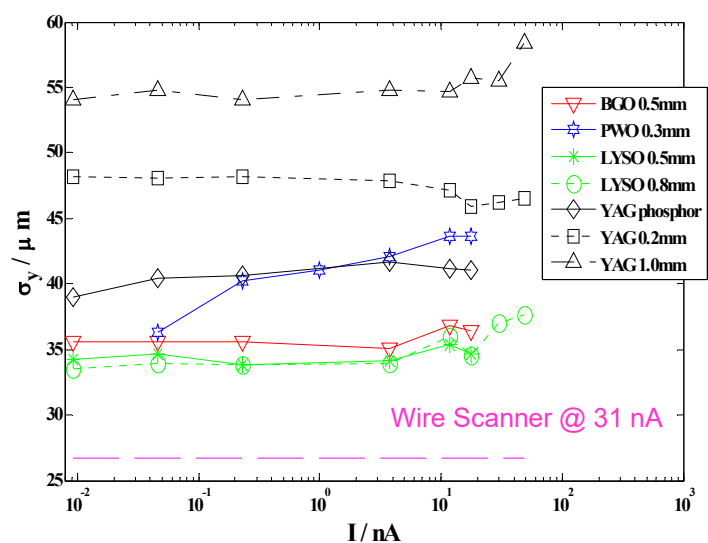


multi-stage emission process:

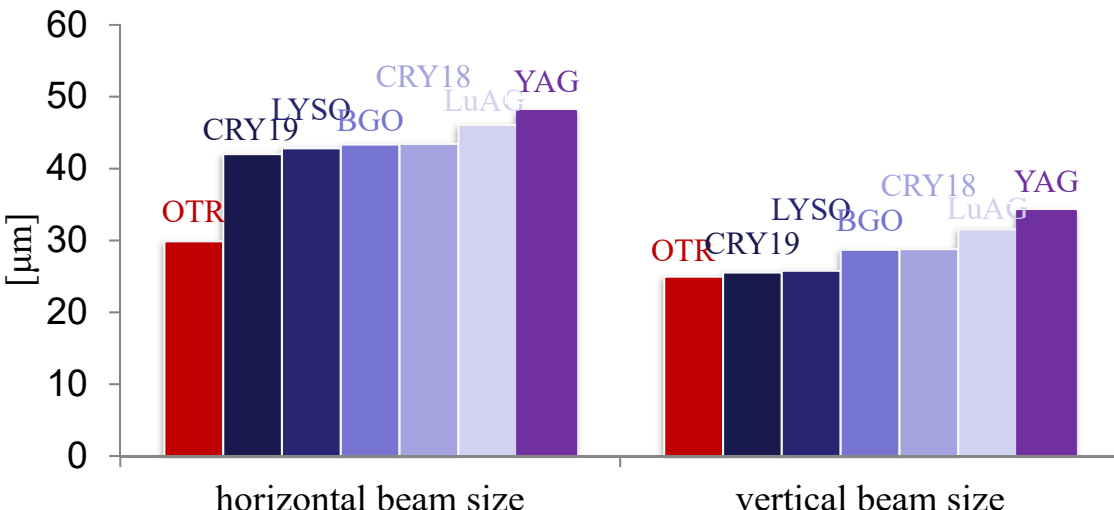
scintillator

LYSO:Ce as Scintillator Material

- series of measurements at Mainz Microtron MAMI (Univ. Mainz, Germany)

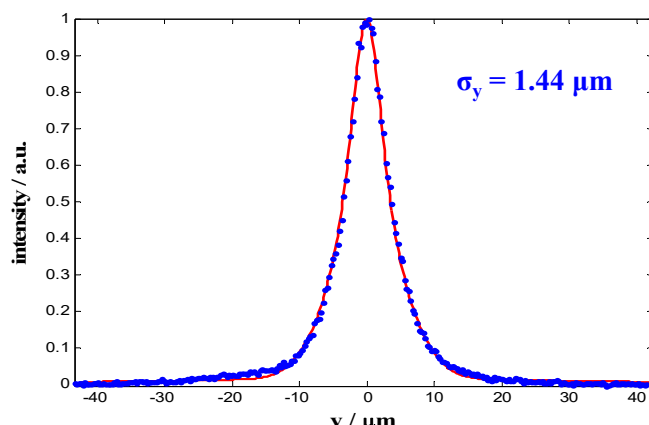
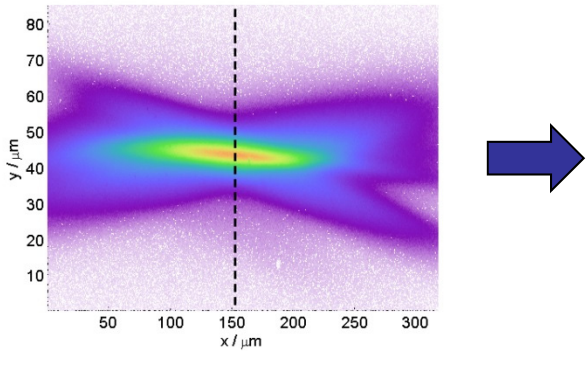


G. Kube et al., Proc. IPAC'10, Kyoto (Japan), 2010, p.906



G. Kube et al., Proc. IPAC'12, New Orleans (USA), 2012, p.2119

- LYSO:Ce best spatial resolution



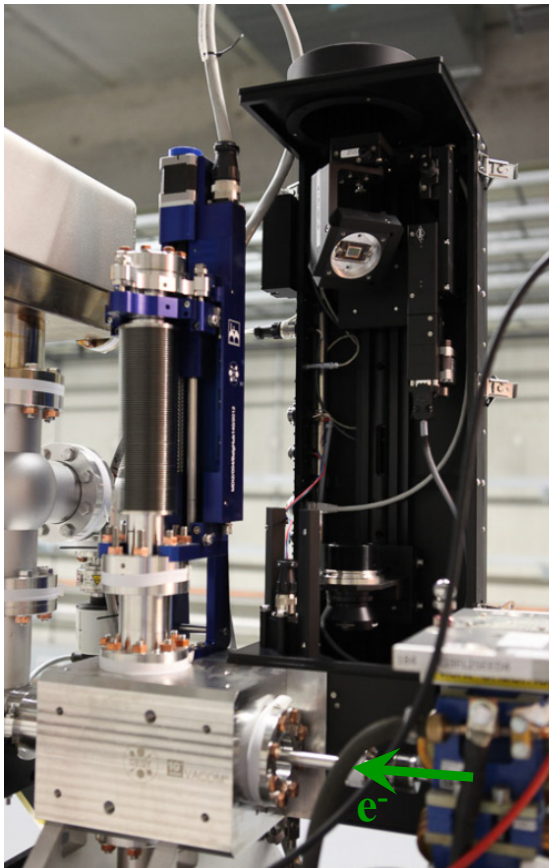
beam size in excellent
agreement with independent
OTR measurement

G. Kube et al., Proc. IBIC'15,
Melbourne (Australia), 2015, p.330

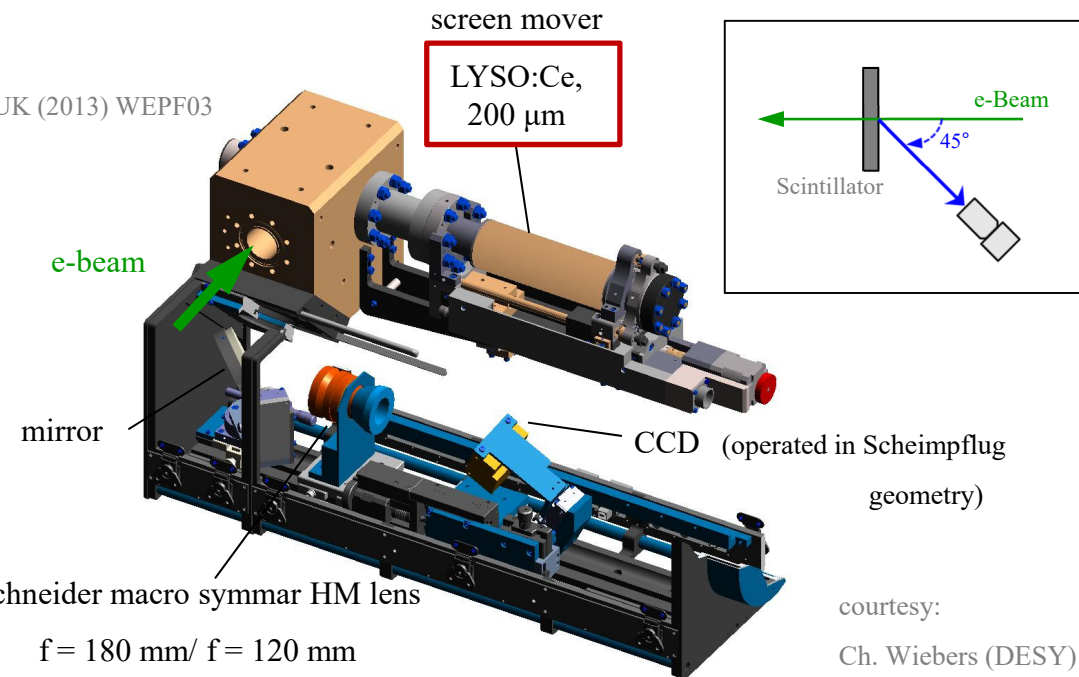
XFEL Screen Monitors

- monitor setup

Ch. Wiebers, M. Holz, G. Kube et al., Proc. IBIC 2013, Oxford, UK (2013) WEPF03



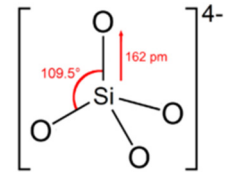
→ ~ 70 monitors in operation



courtesy:
Ch. Wiebers (DESY)

- LYSO:Ce scintillator

- Lutetium Yttrium (Oxi-)Orthosilicate
→ $\text{Lu}_{2(1-x)}\text{Y}_{2x}\text{SiO}_5:\text{Ce}$
- Yttrium: stabilize crystal growth ($x \sim 0.1$)
→ easier and cheaper to grow
→ similar properties than LSO scintillators
- orthosilicate ion: $[\text{SiO}_4]^{4-}$



Beam Profile Observation

- “smoke-ring“ shaped beam profiles @ XFEL

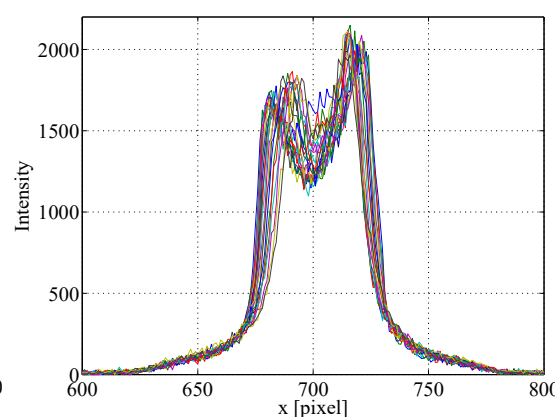
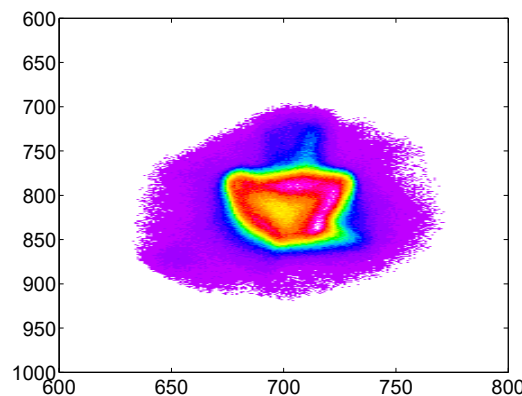
- projected emittances larger than expected

injector: ~ 1 mm.mrad

BC1, BC2: > 2 mm.mrad

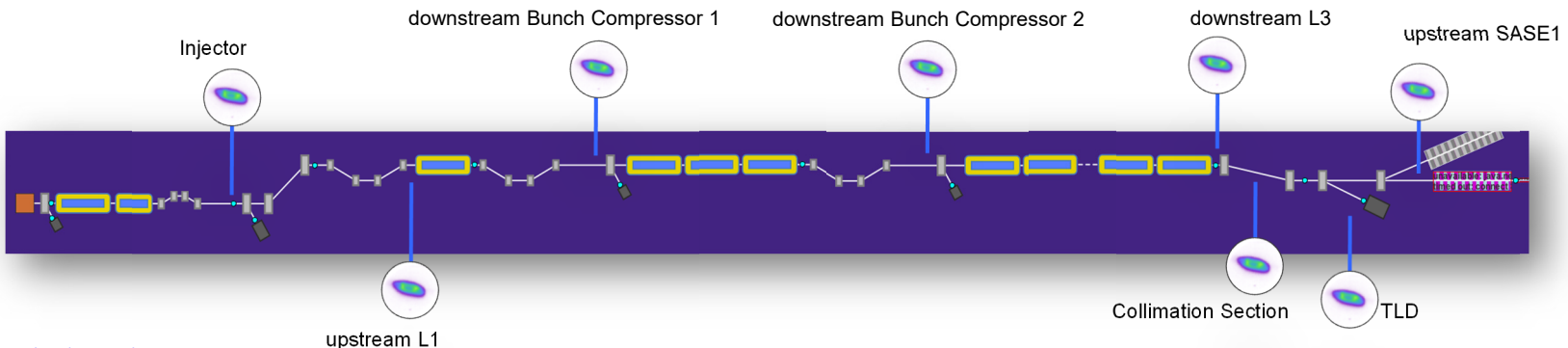
downstream L3: > 4 mm.mrad

- same origin of large emittance and
„smoke-ring“ shaped profiles ?



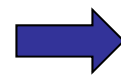
- appear on all screens along the XFEL beamline

courtesy: M. Scholz (DESY)



- excluded options

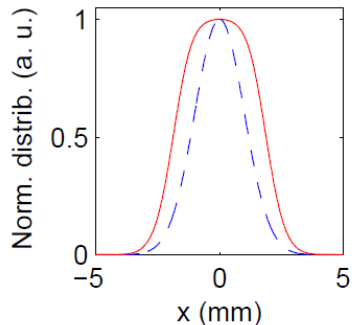
- COTR contribution → linear intensity dependence, stable signal
- space charge effects from gun might lead to depopulation of bunch center
→ should not be visible on all screens (dedicated phase advance required)
- CCD saturation effects



suspicious:
effect of scintillator

Screen Saturation: e⁺/- Beams

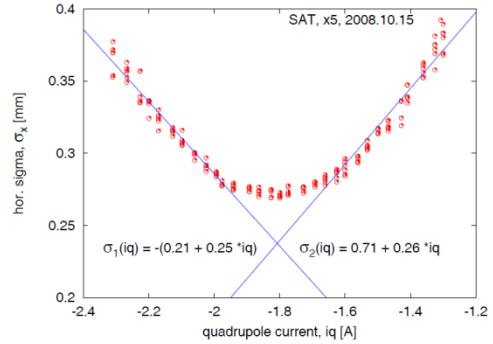
- A. Murokh et al., in *The Physics of High Brightness Beams*, World Scientific (2000), p.564.
- A. Murokh et al., Proc. PAC'01, Chicago, USA (2001) p.1333
- T. F. Silva et al., Proc. PAC'09 , Vancouver, Canada (2009) p.4039



model for saturated beam profiles:

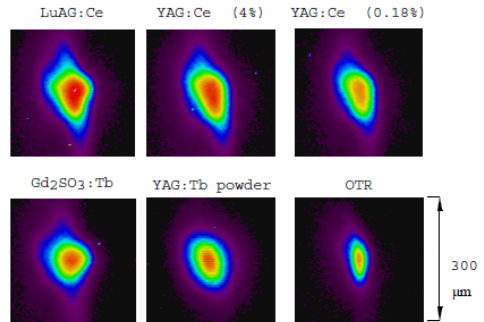
$$I(x) = I_{max} \left[1 - \exp \left(-\frac{1}{\sqrt{2\pi}} \frac{\lambda i_0}{\sigma} \exp \left(-\frac{x}{2\sigma^2} \right) \right) \right]$$

- U. Iriso et al., Proc. DIPAC'09 , Basel, Switzerland (2009), p.200



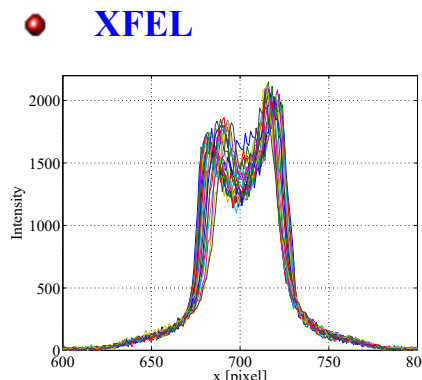
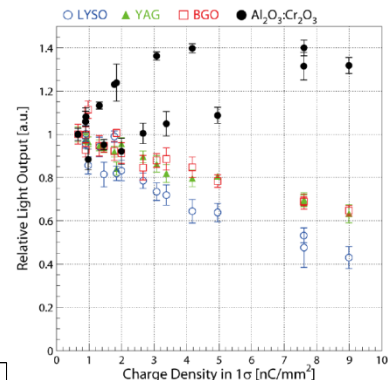
YAG:Ce / OTR
measurements at
ALBA

- R. Ischebeck, FEL'17 Santa Fe, USA (2017) WEP039
saturation of scintillators in profile monitors



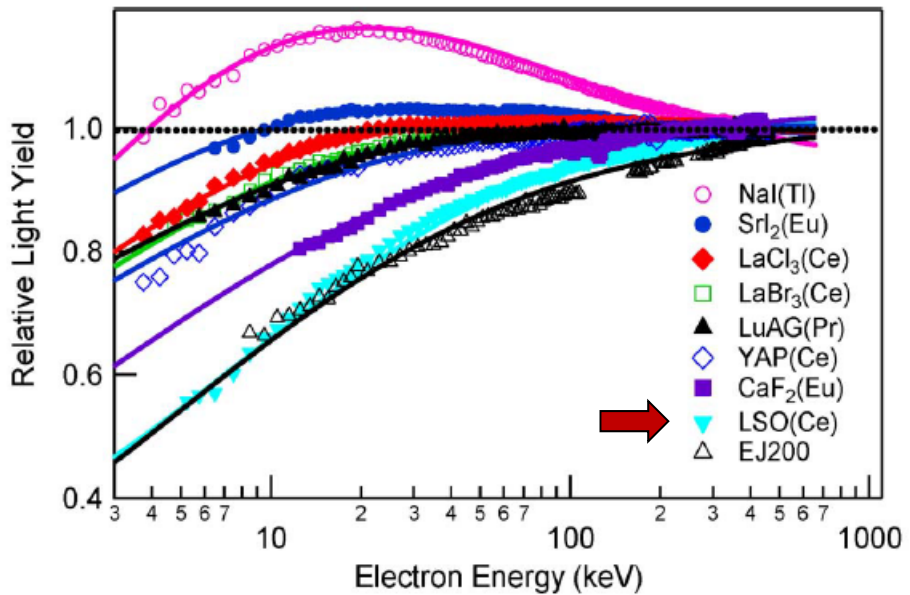
- F. Miyahara et al., Proc. IPAC'17 , Copenhagen, Denmark (2017) p. 268

measurements
at KEK injector
linac



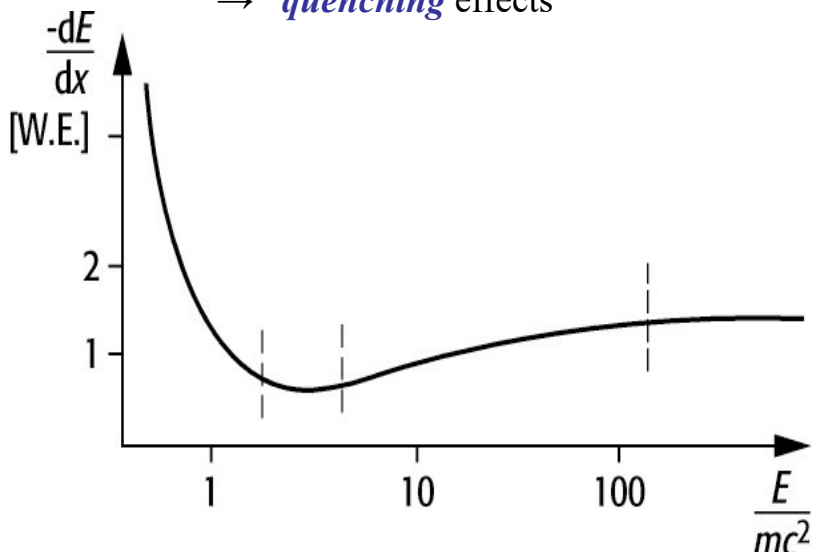
HEP Scintillator Experience

- application of inorganic scintillators in HEP
 - calorimetry
 - non-linearity in energy resolution



S.A. Payne et al., IEEE Trans. Nucl. Sci. **58** (2011) 3392

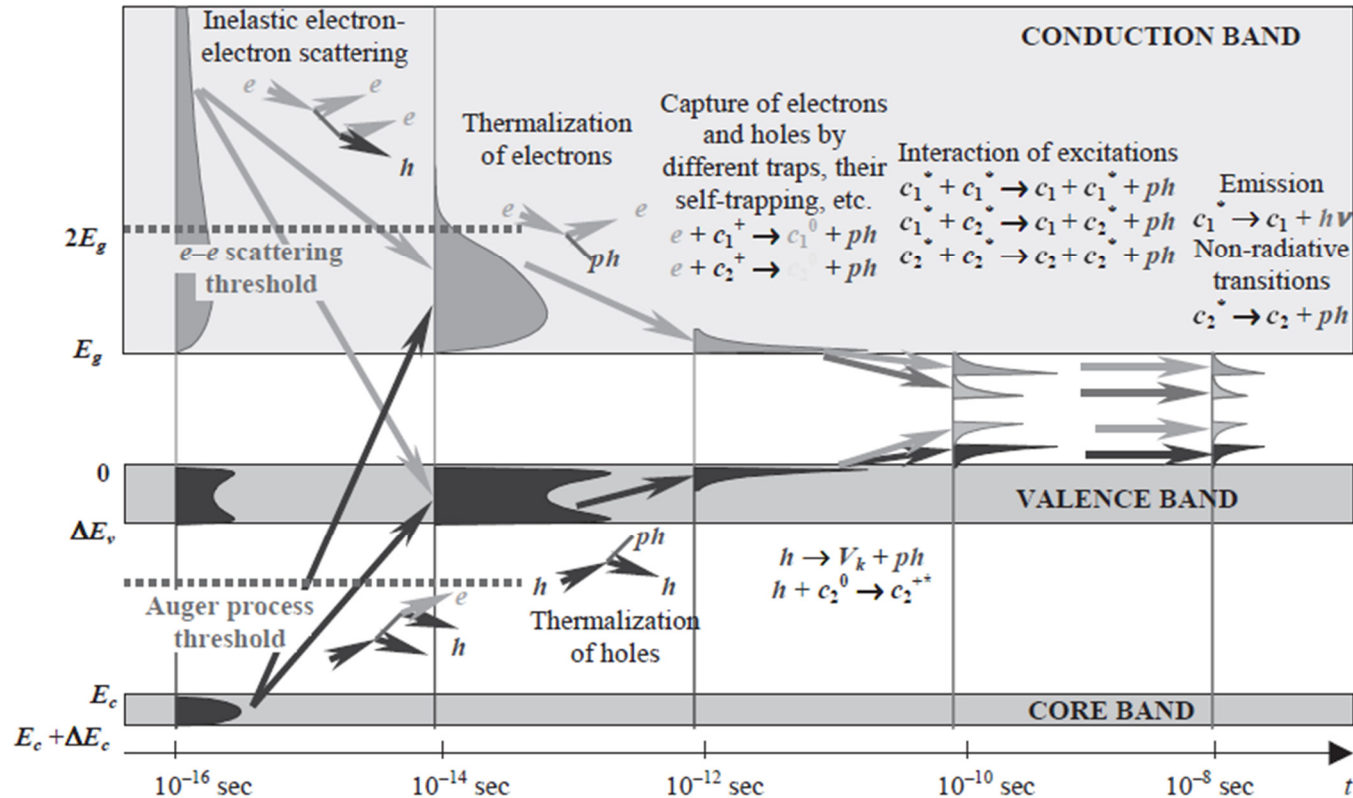
- explanation in terms of energy loss
 - creation of el.magn. shower in target
 - end of shower: low energy particles
 - low energy: high energy loss
 - **high ionization density** in track
 - **quenching** effects



- critical parameter: **ionization density in particle track**
 - resolution studies @ MAMI
 - cw-beam with low charge density
 - XFEL
 - up to 10^{10} particles / bunch

Scintillation Light Generation

- multi stage process



- energy conversion
- thermalization
- localization
- transfer to luminescent centers**
- radiative relaxation

A.N. Vasil'ev, Proc. SCINT'99,
Moscow (Russia), 1999, p.43

- stage responsible for density effects, non-linearity effects, ...

› high density in ionization track (for calorimetry @ low shower particle energies)

→ Auger-like non-radiative recombination of excitation states (e/h pairs, excitons)

quenching

Transfer to Beam Profile Diagnostics

- collisional stopping power
- Fermi plateau:
 - › saturation polarization of target material by particle field
 - › transverse field range → **Fermi radius**

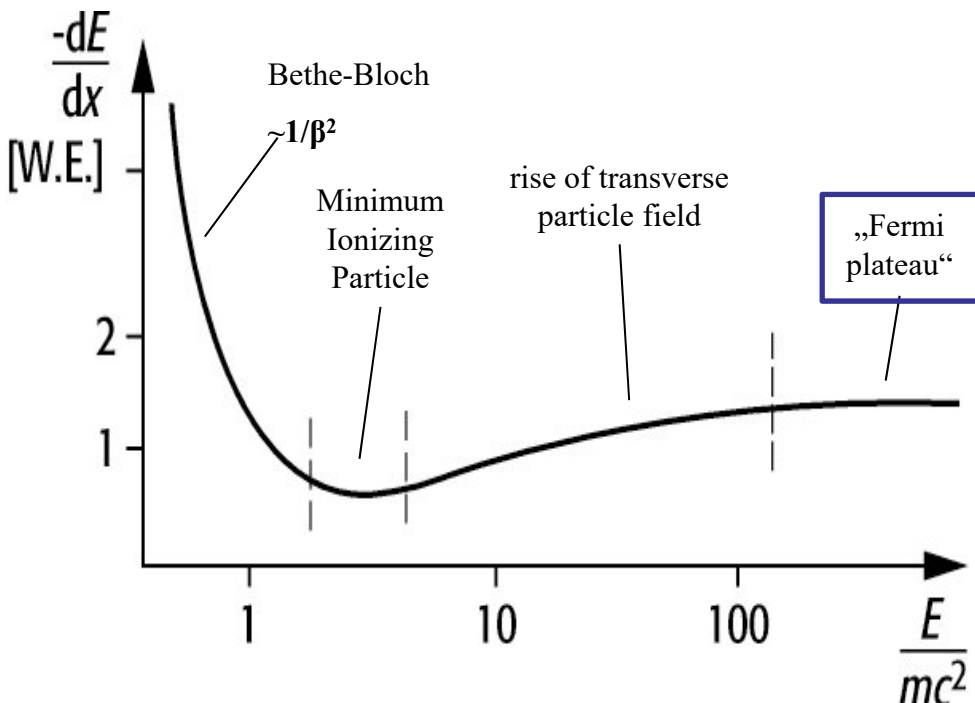
$$R_F = \frac{\hbar c}{\hbar \omega_p}$$

$\hbar \omega_p$: plasma energy

- › R_F : radius of ionization track
→ $R_F(LSO) \sim 3.85 \text{ nm}$

- radiative stopping power (thin targets)
 - › LYSO screen thickness @ XFEL → $t = 200 \mu\text{m}$
 - › Bremsstrahlung mean free path length → $\lambda_{BS} = 1.24 \text{ mm}$
- scintillator non-linearity → ionization track density
 - › beam profile diagnostics: determined by **density of primary beam particles** (ultra relativistic $e^{-/+}$)

→ not by **shower particle energies** (calorimetry for HEP)



Ionization Track Density

- beam interaction with target material (scintillator)

› inelastic scattering (impact ionization): $\sigma_{\text{ion}} \sim E_{\text{kin}}^{-1} \cdot \ln(C \cdot E_{\text{kin}})$
 → energy loss @ Fermi plateau

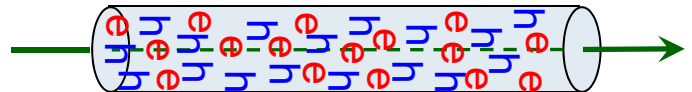
LSO: $\frac{dE}{dx} \approx 1.8 \frac{\text{MeVcm}^2}{\text{g}}$ $\rho = 7.4 \frac{\text{g}}{\text{cm}^3}$  $\Delta E \approx 266 \text{ keV}$

$t = 0.2 \text{ mm}$

- › multiple scattering

LSO: ~ 900 scattering events in 200 μm thick scintillator
 → mean path length between scattering events >> ionization track radius
 ~220 nm >> ~3.8 nm

→ electron passage modeled as *straight tube* of ionization with *radius* R_F



- time scales

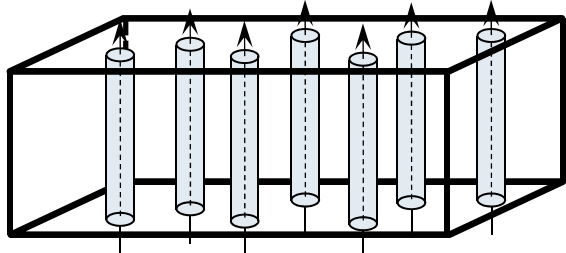
› particle flight time: $< 10^{-12} \text{ s}$ › dynamical processes in scintillator: $10^{-12} - 10^{-10} \text{ s}$
 › bunch lengths (uncompressed): $\sim 10^{-12} \text{ s}$

→ static and homogeneous ionization tube (w.r.t. particle beam dynamics)

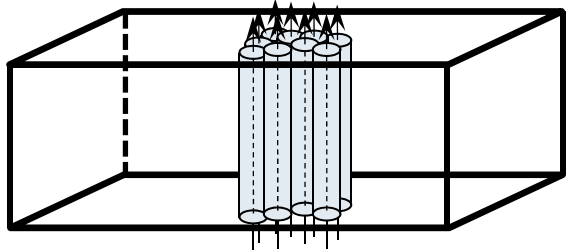
Ionization Track Density (2)

- electron passage through scintillator

 - low charge density beam



 - high charge density beam

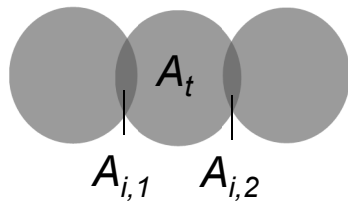
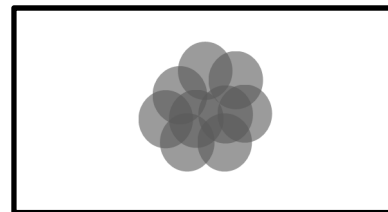
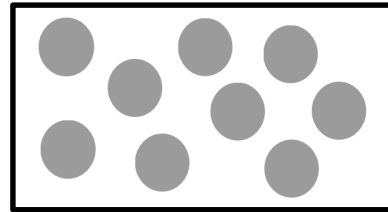


- scintillator non-linearity

 - driven by ionization track density
 - measure for track density
 - area of track circle A_t
 - + area of intersection(s) A_i

static homogeneous ionization tubes:

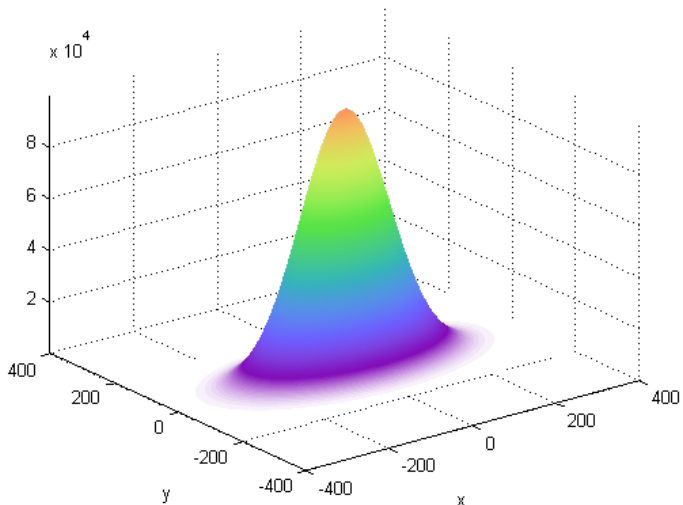
2D representation sufficient



$$n_t \propto A_t + \sum_k A_{i,k}$$

Quenching Model for Beam Profiles

- starting point: Gaussian beam profile



- weight factor for each point of beam profile
 - Birks-type weight factor for scintillator non-linearity

J.B. Birks, Proc. Phys. Soc. **A64** (1951) 874

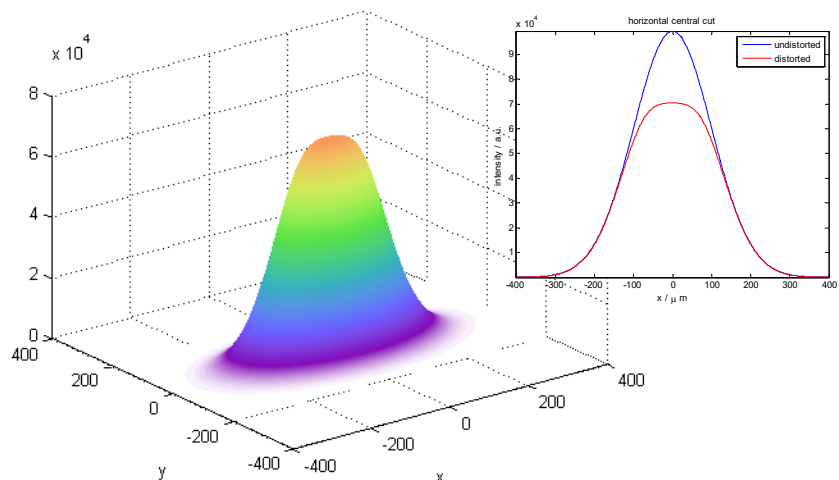
$$w = \frac{1}{1 + \alpha \frac{dE}{dx}}$$

with $\frac{dE}{dx} \propto (n_t)^3$

→ α : free adjustable parameter (quenching strength)

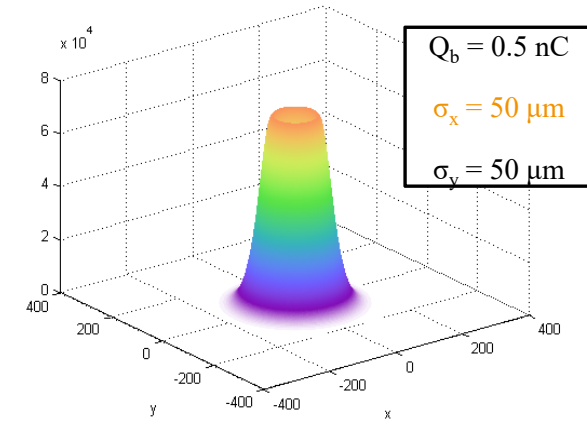
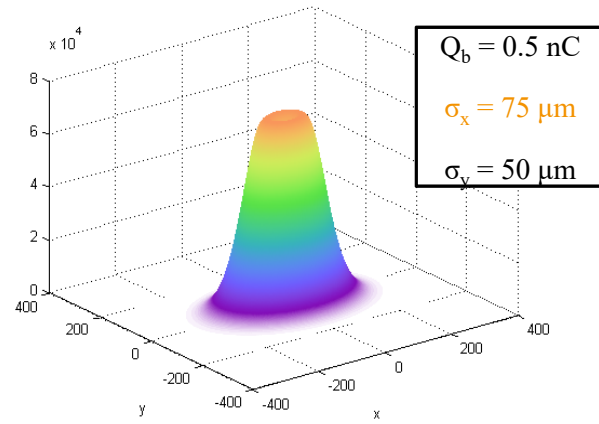
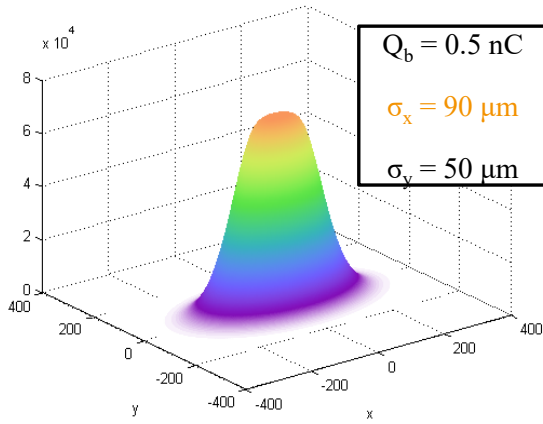
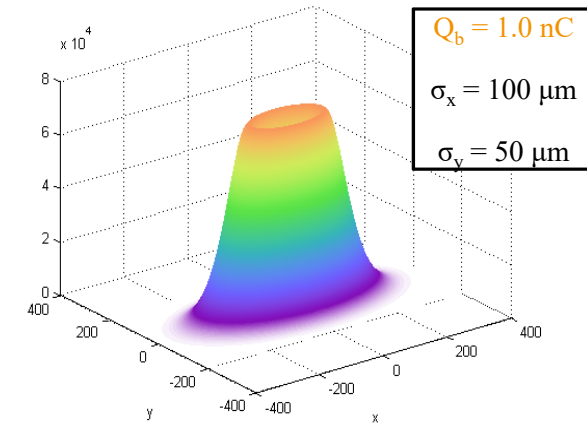
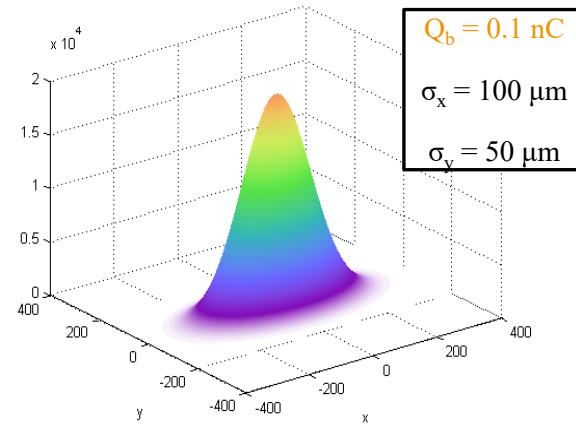
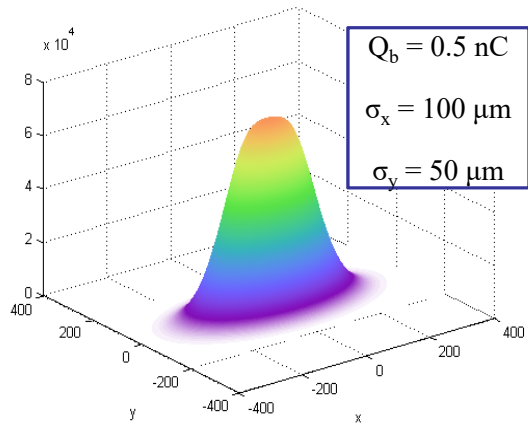
- transform into 2D surface density profile
- derive mean distance between ionization tracks
 - considering nearest neighbour distribution
- calculate measure for ionization track density n_t
 - area of track circle + sum of intersections

- distorted beam profile ($\alpha = 6.4 \times 10^{-5}$)



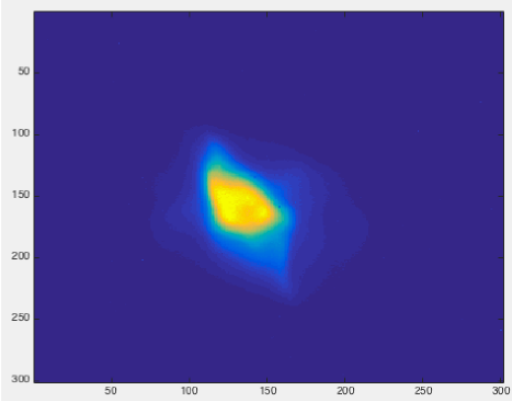
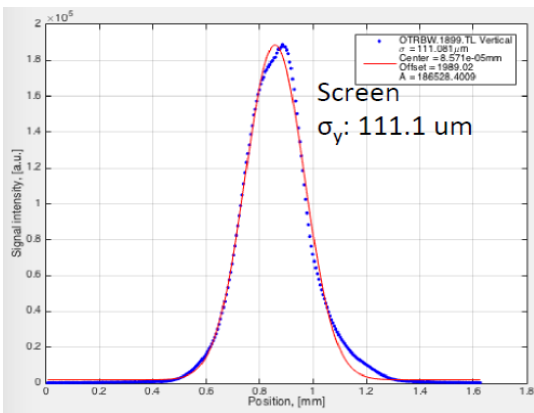
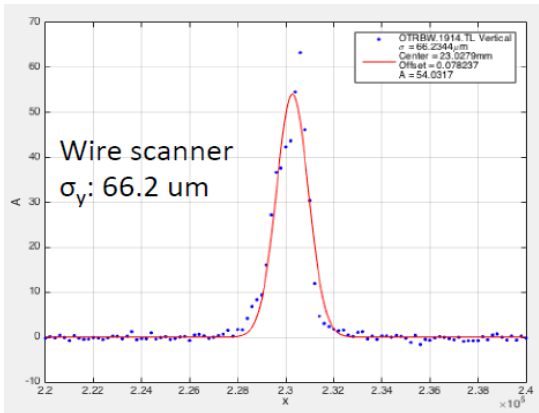
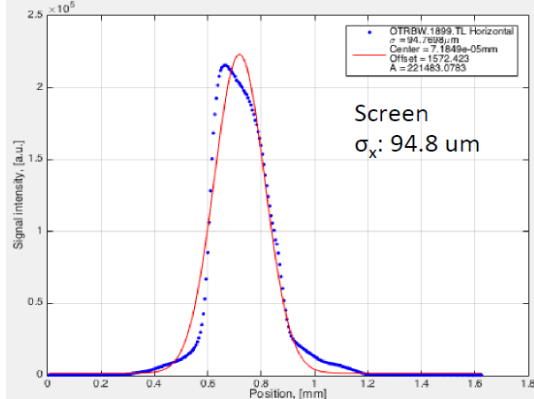
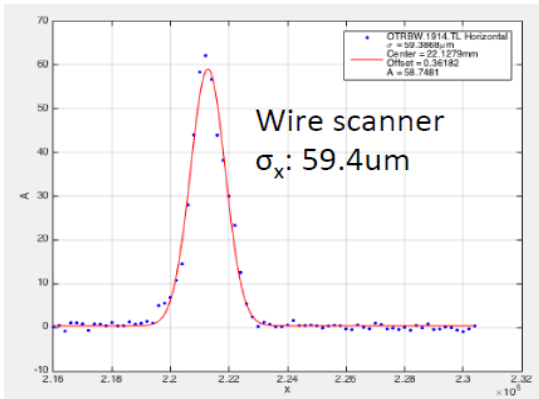
Model Calculations

- starting point



Comparison Screen / Wire Scanner

- screen station OTRBW.1914.TL
 - bunch charge: $Q_b = 500 \text{ pC}$



- model calculation
 - input: 2D-Gaussian with WS beam sizes

- fit projections with Gaussian distribution:

$$\sigma_x = 97 \mu\text{m}, \sigma_y = 108 \mu\text{m}$$

- larger discrepancies with other measurements

Conclusion and Outlook

- XFEL screen monitors: observation of perturbed beam profiles
 - measured emittance values larger than expected
- $\text{Lu}_{2(1-x)}\text{Y}_{2x}\text{SiO}_5:\text{Ce}$ as scintillator material
 - recent studies showed that LYSO has very low Birks parameter α → non-linear light yield
 - property of silicate based scintillators → oxygen is intimately bound to the silicon as a SiO_4^{4-} moiety
- development of quenching model
 - caused by high *ionization track density* due to *primary beam density* → quenching of *excitation carriers*
 - could explain appearance of smoke ring shaped beams
- quest for suitable scintillator material: fall back on experience in HEP
 - Gadolinium-based scintillators
 - expected that charge carriers/excitons rapidly transfer their energy to excited state of gadolinium
 - should improve linearity
 - Yttrium Aluminium Perovskite (YAP)
 - high mobility of excitation carriers → reduced quenching probability



ongoing investigation at DESY (both theoretical and experimental)

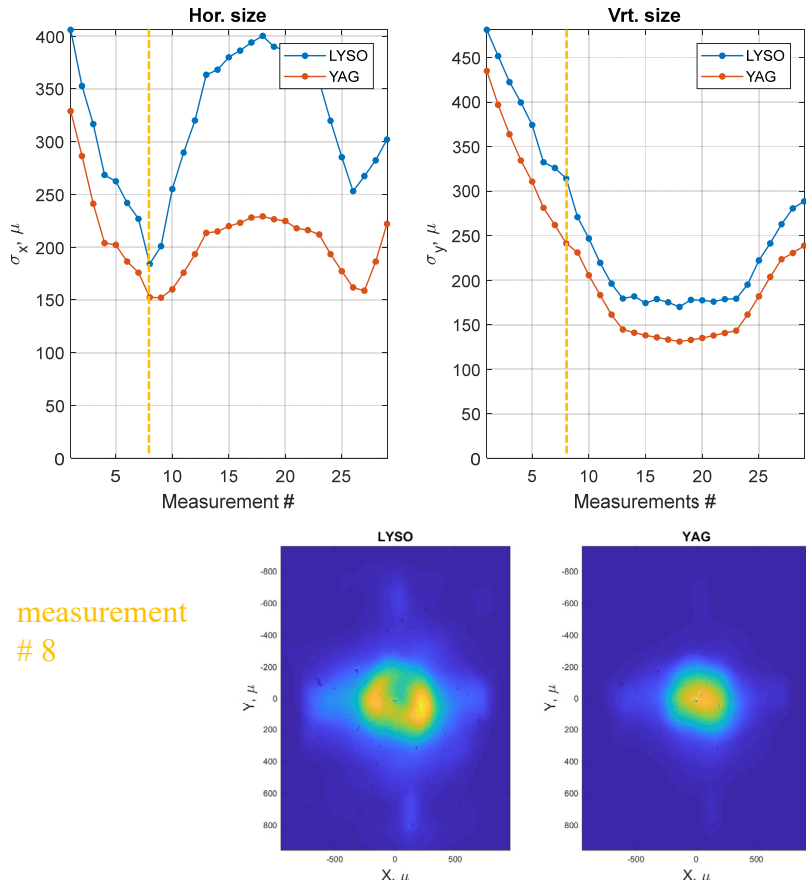
YAG / LYSO Comparison

first test experiments @ XFEL

- both scintillators mounted in screen station OTRBW.1635.L3

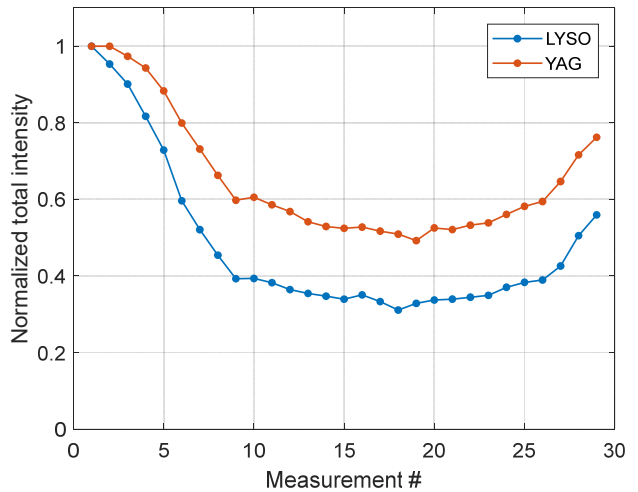
- $E = 14 \text{ GeV}$, $Q_b = 1 \text{ nC}$

- series of measurements → changing beam sizes in both dimensions



measurement
8

- quenching → relative intensity change



- maximum peak charge density

$$\approx 5.3 \frac{\text{fC}}{\mu\text{m}^2}$$

YAP / GAGG and LYSO

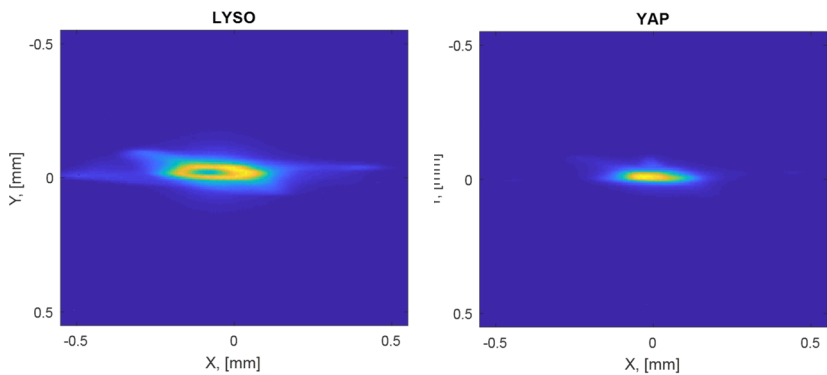
first test experiments @ XFEL

- scintillators mounted together with LYSO in screen stations

- $Q_b = 0.45 \text{ nC}$

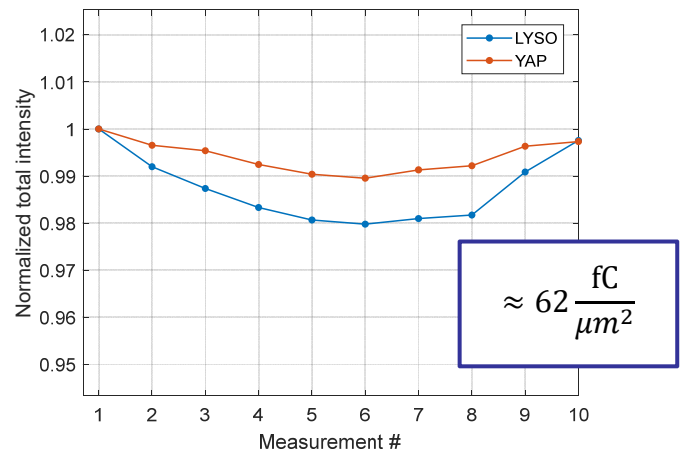
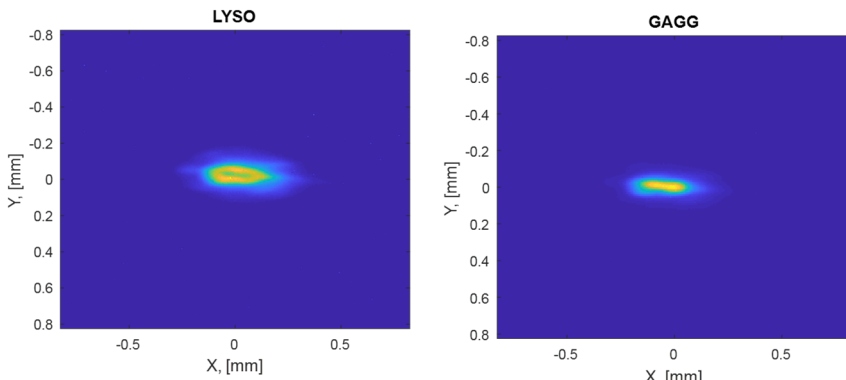
→ beam focussed down in vertical direction

YAP and LYSO



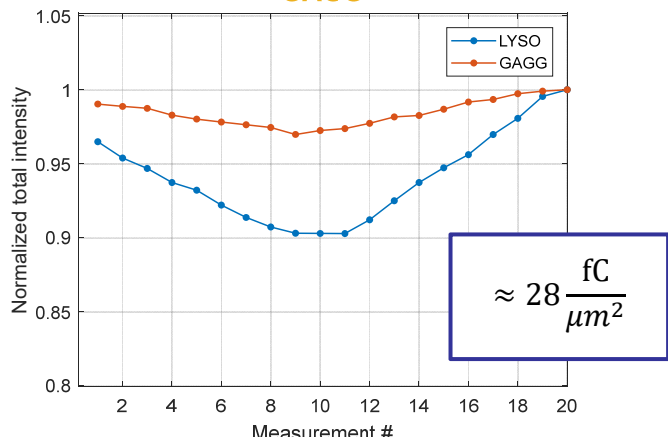
(LYSO: quenching observed already @ measurement #1)

GAGG and LYSO



$$\approx 62 \frac{\text{fC}}{\mu\text{m}^2}$$

GAGG



$$\approx 28 \frac{\text{fC}}{\mu\text{m}^2}$$